Science of the Total Environment 843 (2022) 156777

Contents lists available at ScienceDirect

Science of the Total Environment

journal homepage: www.elsevier.com/locate/scitotenv

Health risk assessment of $PM_{2.5}$ heavy metals in county units of northern China based on Monte Carlo simulation and APCS-MLR

Wenju Wang [a], Chun Chen [b], Dan Liu [b], Mingshi Wang [a,*], Qiao Han [c,d], Xuechun Zhang [a], Xixi Feng [a], Ang Sun [a], Pan Mao [a], Qinqing Xiong [a], Chunhui Zhang [a]

[a] College of Resource and Environment, Henan Polytechnic University, Jiaozuo 454003, China
[b] Henan Key Laboratory for Environmental Monitoring Technology, Zhengzhou 450004, China
[c] Institute of Geochemistry, Chinese Academy of Sciences, Guiyang 550081, China
[d] University of Chinese Academy of Sciences, Beijing 100049, China

HIGHLIGHTS

- Health risk assessment of heavy metals in $PM_{2.5}$ in county-level units
- The coupling of APCS-MLR and HRA based on Monte Carlo simulation is adopted.
- Exposure to Pb and Ni in outdoor is the main cause of human health risk.
- Vehicle emissions and coal burning are identified as major sources of health risk.

GRAPHICAL ABSTRACT

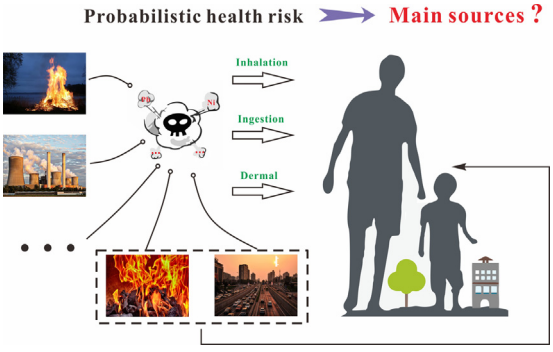

ARTICLE INFO

Editor: Anastasia Paschalidou

Keywords:
$PM_{2.5}$
Heavy metals
Probabilistic health risk
APCS-MLR
County-level population

ABSTRACT

The key areas of China's urbanization process have gradually shifted from urban areas to county-level units. Correspondingly, air pollution in county towns may be heavier than in urban areas, which has led to a lack of understanding of the pollution situation in such areas. In view of this, 236 $PM_{2.5}$ filter samples were collected in Pingyao, north of the Fen-Wei Plain, one of the most polluted areas in China. Monte Carlo simulation was used to solve the serious uncertainties of traditional HRA, and the coupling technology of absolute principal component score-multiple linear regression (APCS-MLR) and health risk assessment (HRA) is used to quantitatively analyze the health risks of pollution sources. The results showed that $PM_{2.5}$ concentration was highest in autumn, 3.73 times the 24 h guideline recommended by the World Health Organization (WHO). Children were more susceptible to heavy metals in the county-level unit, with high hazard quotient (HQ) values of Pb being the dominant factor leading to an increased non-carcinogenic risk. A significant carcinogenic risk was observed for all groups in autumn in Pingyao, with exposure to Ni in the outdoor environment being the main cause. Vehicle emissions and coal combustion were identified as two major sources of health threats. In short, China's county-level population, about one-tenth of the world's population, faces far more health risks than expected.

1. Introduction

$PM_{2.5}$ (particles with an aerodynamic equivalent diameter of less than or equal to 2.5 μm), the main cause of haze events (Liu et al., 2013; Zhang et al., 2016; Qiao et al., 2016), is a mixture of pollutants emitted

* Corresponding author.
E-mail address: mingshiwang@hpu.edu.cn (M. Wang).

http://dx.doi.org/10.1016/j.scitotenv.2022.156777
Received 4 April 2022; Received in revised form 26 May 2022; Accepted 14 June 2022
Available online 18 June 2022

by various potential sources of pollution such as urban construction, automobile exhaust, industrial production, coal combustion, and sand and dust weather under physicochemical action (Kong et al., 2020; Feng et al., 2018; Hahad et al., 2020). The chemical composition of fine particulate matter is complex, each city shows different pollution characteristics according to its energy structure, industrial distribution, and geographical location (Wang et al., 2020). $PM_{2.5}$ not only pollutes the surrounding air environment but can also reduce atmospheric visibility, affect the Earth's radiation budget and global climate change, and even seriously threaten public health (Jena et al., 2019; Cao et al., 2012; Xie et al., 2020). Long-term exposure to fine particulate matter pollution increases the risk of respiratory, cardiovascular and kidney diseases (Beelen et al., 2015; Ran et al., 2020; Cristaldi et al., 2022; Copat et al., 2020; Dastoorpoor et al., 2019), even causing about 4.2 million premature deaths each year (Cohen et al., 2017). The serious risk of $PM_{2.5}$ to humans has attracted extensive attention.

Fine particulate matter is characterized by a small volume and large specific surface area, and can easily absorb many harmful substances in the environment, among which heavy metals are important pollutants that cause human health risks due to their toxicity and enrichment (Guo et al., 2020a; Lai et al., 2015). Previous studies have shown that heavy metals occupy only a small fraction of $PM_{2.5}$, but can contribute to a variety of diseases because of their association with mitochondrial damage and induction of oxidative stress (Ghasemi et al., 2020; Idani et al., 2020). In recent years, pollution characteristics, source analysis, and ecological and health risks of different heavy metals in $PM_{2.5}$ have become a research hotspot (Abuduwailil et al., 2015; Ye et al., 2018; Ogundele et al., 2017). The source analysis of fine particles is mainly based on the receptor model. Absolute principal component score-multiple linear regression (APCS-MLR), a reverse traceability method, can quantify the contribution rate of all pollution sources without constructing the component spectrum of pollution sources, which is more efficient than principal component analysis (PCA) and traditional chemical mass balance (CMB). Heavy metal risk assessment generally consists of four processes: identification of hazardous chemical species, variation in adverse effects owing to different doses, calculation of exposure, and quantitative characterization of risk (Mohammadi et al., 2018). Currently, research on the health risk of heavy metals in $PM_{2.5}$ relies too much on the health risk assessment (HRA) model with definite parameter values while ignoring the limited availability of heavy metal samples and the different parameter characteristics of different populations and individuals, such as differences in body weight and duration of heavy metal exposure. This could underestimate or overestimate the health risks (Hu et al., 2017; Huang et al., 2021). Fortunately, Monte Carlo simulation is a statistical method based on probabilistic and statistical theory to analyze uncertainties and identify the proportion of population health risks above non-carcinogenic and carcinogenic thresholds by fitting the probability distributions of parameters to ensure the accuracy of health risk assessment. It has been widely used in health risk assessment of heavy metals (Yang et al., 2019; Chen et al., 2019a; Huang et al., 2021; Goudarzi et al., 2018).

Most of the existing studies have been carried out in urban areas because of the high level of socio-economic development, high population density, and industrial concentration. However, studies on typical small-scale high-precision county-level units have been neglected. Over the past decade, >50 % of China's new urban population has been in county-level units. The focus of urbanization has shifted from cities to surrounding counties, and county-level unit urbanization is a long-term trend (Su, 2021). There are more potential pollution sources in surrounding counties than in urban areas. Additionally, counties are subject to lower environmental supervision than urban areas, and county-level units may have a higher burden of air pollution than urban areas (Li et al., 2018; Zhi et al., 2017). Haze pollution has trended downwards on time scales significantly in the vast majority of China's 27 major cities, such as Beijing, Nanjing and Zhengzhou (Li et al., 2021). In contrast, the annual average $PM_{2.5}$ mass increased from 29.52 $\mu g/m^3$ to 42.83 $\mu g/m^3$ between 2000 and 2010 in 2640 county-level units in China (Han et al., 2021a), a trend that has continued in recent years (Li et al., 2019; Chen et al., 2018). Permanent residents in China's county region totaled 745 million in 2020, and about one-tenth of the global population is suffering from health threats caused by $PM_{2.5}$ exposure. There is an urgent need to study a typical county and quantify the health risks of residents in county-level units.

The Fen-Wei Plain, one of the areas severely afflicted by haze in China, was first listed as the key control area of the “Blue Sky Protection Campaign” by the Ministry of Ecology and Environment of the People's Republic of China in 2018. Coal accounts for 90 % of the primary energy consumption structure in most areas of the Fen-Wei Plain, which is much higher than the 80 % in the Beijing-Tianjin-Hebei region during the peak coal consumption period (Dong et al., 2021). In addition to the pollutant emissions of coal during combustion, it also relies excessively on the road system during transportation, which results an increased burden on local transportation and high vehicle exhaust pollution (Chen et al., 2019a,b; Dong et al., 2021). There are many high coal-consuming enterprises, such as thermal power and coking in the Fen-Wei Plain, with heavy industrial structures and large emissions of industrial pollutants. Pingyao County, located in the north of the Fen-Wei Plain, was considered the target area in this study, with Pingyao being bordered by the Lvliang Mountains to the north and the Taihang Mountains to the south. It is worth mentioning that the ancient city of Pingyao, a world cultural heritage site, is located in the north of the county, and there are many tourists every day, which means that motor vehicle emissions in the study area may not be optimistic. Pollutants emitted by coal combustion and vehicle emissions tend to accumulate owing to the blocking of mountains and the influence of downdrafts on leeward slopes, resulting in severe local haze events. APCS-MLR was used for source identification and allocation of heavy metals in $PM_{2.5}$. In addition, APCS-MLR in combination with HRA was utilized to enable health risk assessment based on concentration values and sources, providing a scientific basis for reducing heavy metal exposure in atmospheric fine particulate matter and pollution control.

2. Materials and methods

2.1. Study area and sample collection

Pingyao is (112°12E to 112°31E, 37°12N to 37°21N) located in the north of the Fen-Wei Plain, with an area of 1260 km^2, which is a county in central Shanxi Province (Fig. 1). It belongs to the monsoon climate of medium latitudes, with an average annual temperature of 10.6 °C. Factories, enterprises, and farmland are mostly in rural areas or suburbs, whereas commercial and residential areas are mostly in urban areas.

Sampling points were chosen according to the “Technical Methodological Guidelines for Ambient Air Particle Source Analysis Monitoring” issued by the Chinese Ministry of Ecology and Environment in 2020. In this study, the Pingyao County People's Government was selected as the sampling site (112°18′E, 37°19′N) (on the rooftop of the party and government building) to collect $PM_{2.5}$ samples during four seasons, because it is surrounded by residential buildings, commercial areas and urban roads, and belongs to a typical mixed commercial and residential area, which can accurately reflect the overall situation of air pollution in Pingyao. $PM_{2.5}$ samples were collected from July 2020 to June 2021 on 90 mm diameter PTFE filters (Tianjin Jinhai Environmental Protection Technology Co., Ltd., China) by using a specific medium flow rate (0.96 ± 0.04 L/min) KDB-120B sampler (Qingdao Kedibo Electronic Technology Co., Ltd., China). Before sampling, all filters were heated at high temperatures (120 °C) for 2 h, then placed in a glass desiccator to equilibrate the moisture for 24 h. $PM_{2.5}$ samples were collected twice a day, from 8 a.m. to 8 p.m. and from 8 p.m. to 8 a.m. the next day. In total 236 effective samples were collected. The sampling times were as follows: a. Summer (57 effective samples): 31 July–31 August 2020, b. Autumn (60 effective samples): 20 October–3 November 2020, 16 November–2 December 2020, c. Winter (60 effective samples): 5 January-3 February 2021, d. Spring (59 effective samples): 8 May-22 June 2021. All $PM_{2.5}$ samples collected were stored in a refrigerator (−18 °C) until chemical analysis was performed in the laboratory. Heavy metal analysis and quality control are provided in the Supplementary Material.

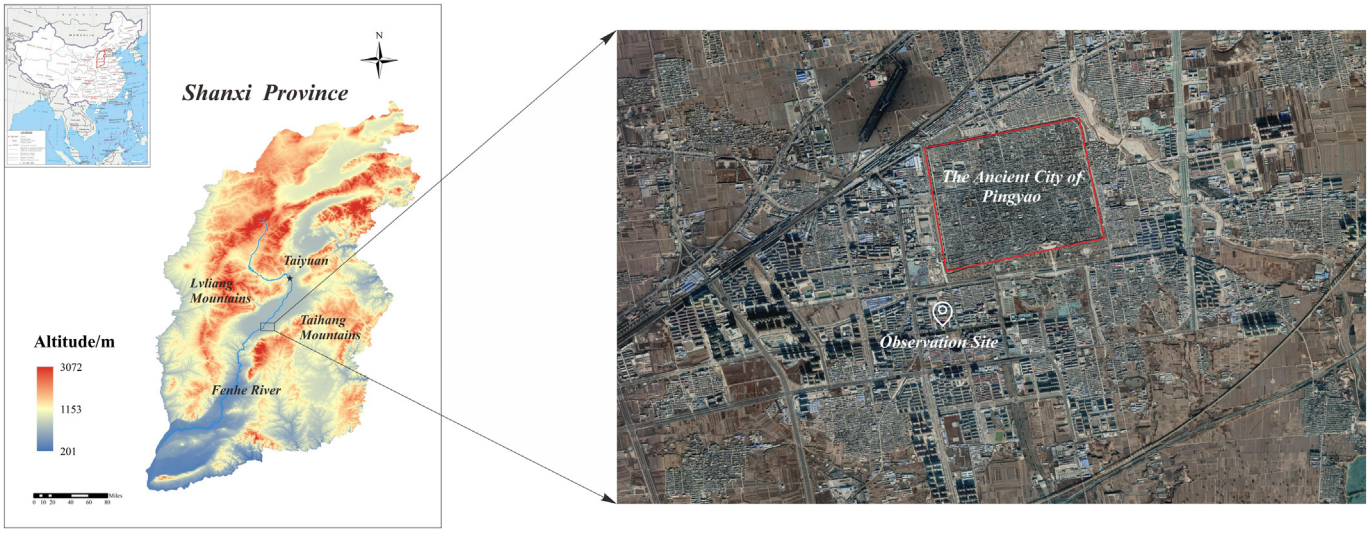

Fig. 1. Geographical location map of sampling site.

2.2. Evaluation of heavy metals pollution

The enrichment factor (EF) method has been widely used to study the enrichment degree of heavy metals in atmospheric fine particulate matter, which can be used to judge and evaluate the impact of human production activities on the natural environment (Li et al., 2018). The calculation formula of the EF is as follows:

$$EF = \frac{(C_i/C_n)_{aerosol}}{(C_i/C_n)_{crust}} \quad (1)$$

where C_i is the mass concentration of each element (μg/m^3), C_n is the mass concentration of the reference element (μg/m^3), $(C_i/C_n)_{aerosol}$ represents the ratio of the ith element to the selected reference element in the aerosol, $(C_i/C_n)_{crust}$ represents the ratio of the ith element to the selected reference element in the crust. Al was selected as the reference element, and its concentration in the crust was referenced to the a-layer soil in Shanxi Province, China (SEPA, 1990). This study divided EF into three grades, slightly enriched ($5 < EF \leq 10$), moderately enriched ($10 < EF \leq 60$), and severely enriched ($EF > 60$).

2.3. PCA-APCS-MLR

PCA is a widely used data dimension reduction algorithm that can select a small number of important variables through linear transformation to minimize the loss of original information. However, PCA is usually used only to determine the types and quantities of potential pollution sources. APCS-MLR converts standardized principal factor scores into non-standardized absolute principal factor scores on the basis of PCA and then quantitatively estimates the contribution rate of pollution sources to each pollutant using multiple linear regression (Zhang et al., 2020; Jin et al., 2019; Thurston and Spengler, 1985). The conversion process from the principal factor scores to the absolute principal factor scores in the APCS-MLR receptor model is as follows:

$$(Z_0)_j = \frac{0 - \overline{C_j}}{\sigma_j} \quad (2)$$

$$(A_0)_k = \sum_{j=1}^{j} S_{kj} \times (Z_0)_j \quad (3)$$

$$APCS_k = (A_z)_k - (A_0)_k \quad (4)$$

where $(Z_0)_j$ is the standardized value when the concentration of the pollutant is set to zero, $\overline{C_j}$ is the average concentration of the pollutant, σ_j is the standard deviation of the pollutant concentration. $(A_0)_k$ is the principal component score under the absolute zero value; $(A_z)_k$ is the score value of the principal component; $APCS_k$ is the absolute principal factor score. Finally, the contribution of pollution sources to each pollutant was estimated using the following linear regression equation:

$$C_j = \sum_k a_{kj} \times APCS_k + b_j \quad (5)$$

where a_{kj} is the multiple linear regression coefficient of pollutant j from source k, b_j is the constant term of a linear equation of many variables.

The results showed negative values when we used the PCA-APCS-MLR model to calculate the contribution rate of pollution sources, which led to a deviation in the calculation result of the contribution rate. To ensure the reliability of the calculation results, an absolute function was used to convert all negative values into positive ones (Gholizadeh et al., 2016).

2.4. Health risk assessment (HRA)

The possible non-carcinogenic and carcinogenic risks caused by heavy metals in $PM_{2.5}$ were evaluated using the health risk assessment model recommended by USEPA (2011). Heavy metals in $PM_{2.5}$ are mainly harmful to human health through ingestion (ADD_{ing}), inhalation (ADD_{inh}), and dermal absorption (ADD_{derm}). The formula for the daily exposure to these three pathways is as follows:

$$ADD_{ing} = \frac{C \times IngR \times EF \times ED \times CF}{BW \times AT} \quad (6)$$

$$ADD_{inh} = \frac{C \times InhR \times EF \times ED}{BW \times AT \times PEF} \quad (7)$$

$$ADD_{derm} = \frac{C \times SA \times SL \times ABS \times EF \times ED \times CF}{BW \times AT} \quad (8)$$

where C represents the concentration of heavy metals (mg/kg), *IngR* is the ingestion rate (mg/day), EF is the exposure frequency (day/year), ED is the exposure duration (years), CF is the conversion coefficient 1.0×10^{-6} (kg/mg), BW is the standard body weight (kg), AT is the average exposure time (day), *InhR* is the inhalation rate (m^3/day), PEF is the particulate emission factor (m^3/kg), SA is the skin exposed area (cm^2/day), and SL is the skin adherence factor (mg/cm^2). ABS is the skin absorption factor.

Health risks include non-carcinogenic and carcinogenic risks. Non-carcinogenic risks are measured by the hazard quotient (HQ), and hazard

index (HI) is the sum of the hazard quotient of heavy metals, as shown in the following equation:

$$HQ = \frac{ADD_x}{RfD} \quad (9)$$

$$HI = \sum HQ_i \quad (10)$$

where ADD_x is the average daily intake ($mg \cdot kg^{-1} \cdot d^{-1}$). *RfD* is the corresponding reference toxicity threshold dose ($mg \cdot kg^{-1} \cdot d^{-1}$). If *HQ* or *HI* < 1, there is no non-carcinogenic risk, whereas *HQ* or *HI* ≥ 1, adverse health effects may occur (Ma et al., 2018; Zhang et al., 2018).

Carcinogenic risk (CR) and total carcinogenic risk (TCR) are calculated using the following equation:

$$CR = ADD_x \times SF \quad (11)$$

$$TCR = \sum CR_i \quad (12)$$

where *SF* is the cancer slope factor ($kg \cdot d \cdot mg^{-1}$). If $CR > 10^{-4}$, the risk of cancer is significantly increased, if $10^{-6} < CR < 10^{-4}$, it indicates an acceptable risk of cancer; and if $CR < 10^{-6}$, it is considered to pose little health risk (Ma et al., 2018; Fryer et al., 2006).

Co, Cr, Cu, Mn, Ni, Pb, and Zn were used to assess the non-carcinogenic risks in this study. The International Agency for Research on Cancer (IARC, 2016) classified Cr (VI) and Ni into group 1, Pb into group 2A, Co into group 2B, and Mn, Cu, and Ca were not found to be carcinogenic to the human body. The concentration ratio of Cr (VI) to Cr (III) was approximately 1:6; therefore, the concentration of Cr (VI) was calculated according to 1/7 of the total Cr (Massey et al., 2013). The carcinogenic risks of Cr (VI), Pb (through ingestion and inhalation), Ni (through ingestion), and Co (through inhalation) were also estimated.

2.5. Monte Carlo simulation

The Monte Carlo simulation was implemented using the Crystal Ball software v11.1.24 (Oracle, USA). In this study, the mass concentration data of Co, Cr, Cu, Mn, Ni, Pb, and Zn for four seasons were fitted to the probability distribution, and the health risks of heavy metals were simulated 10,000 times by defining assumptions and predictions.

3. Results and discussion

3.1. Seasonal pollution characteristics of $PM_{2.5}$ and heavy metals

The concentration of $PM_{2.5}$ in Pingyao in the four seasons is shown in Fig. 2. Daily standard values recommended by China and WHO were considered to define the $PM_{2.5}$ pollution levels in Pingyao. However, the classification based on Chinese standard values can more clearly reflect the characteristics of $PM_{2.5}$, compared to the WHO, because of the high $PM_{2.5}$ load in Pingyao. Based on the Technical Regulation on Ambient Air Quality Index (on trial) (HJ633–2012) of China, the $PM_{2.5}$ pollution levels were divided into five categories. Excellent, $PM_{2.5} < 35\ \mu g/m^3$, Good, $35\ \mu g/m^3 \le PM_{2.5} < 75\ \mu g/m^3$, Mild pollution, $75\ \mu g/m^3 \le PM_{2.5} < 115\ \mu g/m^3$, Moderate pollution, $115\ \mu g/m^3 \le PM_{2.5} < 150\ \mu g/m^3$, Heavy pollution, $PM_{2.5} > 150\ \mu g/m^3$. During the monitoring period, the average concentration of $PM_{2.5}$ was 73.88 ± 51.18 $\mu g/m^3$, far higher than the national air quality environmental standard (GB 3095–2012) (annual average level II, 35 $\mu g/m^3$). Compared with other cities in China, it was higher than Kunming (31 $\mu g/m^3$) (Guo et al., 2020b), lower than Taiyuan (83.8 $\mu g/m^3$) (Zhang et al., 2019), Beijing (114.17 $\mu g/m^3$) (Li et al., 2018) and Baoding (93.91 $\mu g/m^3$) (Yan et al., 2018), and close to Handan (75.81 $\mu g/m^3$) (Yan et al., 2018) and Tangshan (72.84 $\mu g/m^3$) (Yan et al., 2018). This indicates that the air pollution burden of county-level units in China is comparable to that of some industrial cities. The concentration of $PM_{2.5}$ in Pingyao showed obvious seasonal variation. The mass of fine particulate matter in spring, summer, autumn, and winter was 63.60 ± 26.71 $\mu g/m^3$, 46.53 ± 26.07 $\mu g/m^3$, 93.13 ± 53.33 $\mu g/m^3$, 90.72 ± 68.92 $\mu g/m^3$, respectively. About 60 % of the autumn samples were higher than the national air quality standard (GB 3095–2012) (daily average level II, 75 $\mu g/m^3$), and the average concentration of fine particulate matter was the highest, which differs from previous studies (Guo et al., 2021; Xie et al., 2019). There are two reasons for this phenomenon. First, heating began in Pingyao on 1 November, and half of the samples collected during the autumn monitoring period were collected after heating, when the amount of coal burning increased and more coal dust entered the atmosphere. Second, low wind speed, high humidity, and special terrain promoted the growth of $PM_{2.5}$. The meteorological data collected during the monitoring period are shown in Table S1.

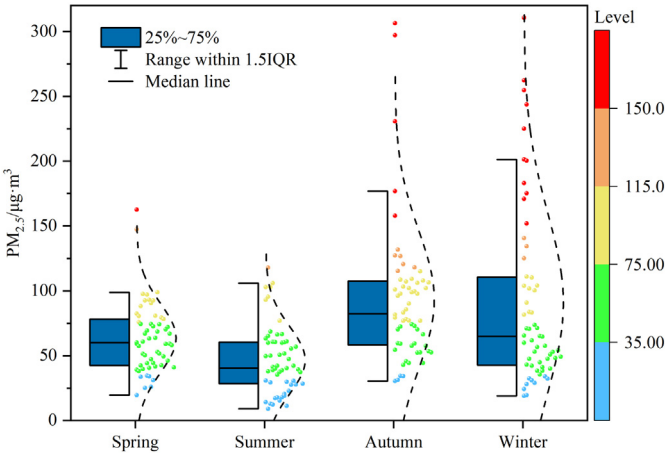

Fig. 2. Seasonal variation of $PM_{2.5}$ concentration and samples distribution statistics.

The descriptive statistics of heavy metals in $PM_{2.5}$ are shown in Table 1. The seasonal variation characteristics of heavy metals were similar to those of fine particulate matter, with the highest average concentration in winter, followed by autumn, spring, and summer. The annual average concentrations of heavy metals from high to low were Ca, Al, Fe, K, Na, Mg, Zn, Pb, Mn, Co, Cu, Ni, and Cr, among which Ca, Al, Fe, K, Na, and Mg were the elements with the highest content in $PM_{2.5}$. The high concentrations of crustal elements may be related to sand-wind weather and construction sites (Wang et al., 2013). The analysis of the other seven heavy metals shows that the average concentration of Zn was the highest, which is 251.8 ± 241.5 ng/m^3, followed by Pb (118.1 ± 240.9 ng/m^3), Mn (80.8 ± 76.7 ng/m^3) and Co (69.0 ± 477 ng/m^3). The concentrations of Cu, Zn, Mn and Ni in autumn were much higher than those in other seasons, and the Cu content was an order of magnitude higher than that in other seasons. Cu and Zn are widely used in the manufacture of tires and brake pads (Banerjee et al., 2015; Han et al., 2020), indicating that Pingyao contributed significantly to vehicle emissions in autumn. In general, the pollution characteristics of heavy metals in the four seasons were very similar; the sources of heavy metals in $PM_{2.5}$ in Pingyao were consistent throughout the year.

3.2. Pollution evaluation of heavy metals

To identify the impact of human activities on heavy metals in $PM_{2.5}$, the EF was used to evaluate the pollution level of heavy metals (Table S2). In spring, Cu, Ni, and Zn were moderately enriched, whereas Co and Pb were severely enriched. In summer, Cu and Ni were moderately enriched, whereas Co, Pb, and Zn were severely enriched. In autumn, Cr and Mn were slightly enriched; Ni was moderately enriched; Co, Cu, Pb, and Zn were severely enriched. In winter, Ni was slightly enriched; Cr, Cu, and Zn were moderately enriched; and Co and Pb were severely enriched. The EF of heavy metals in $PM_{2.5}$, was generally higher in autumn, indicating that human activities play an important role in the high accumulation of heavy metals during this season. The EF of Pb, Co, and Zn were the highest throughout the year, indicating that these elements were seriously affected by anthropogenic sources. Pb, Co, and Zn in fine particulate matter in

Table 1
Summary statistics of heavy metal concentrations in $PM_{2.5}$ in Pingyao (ng/m^3).

Season	Al	Ca	Co	Cr	Cu	Fe	K	Mg	Mn	Na	Ni	Pb	Zn
Spring													
Mean	2336.8	3161.8	47.8	8.6	24.1	1745.9	735.9	551.5	48.9	426.5	16.8	74.0	166.3
Median	1602.4	2008.1	20.5	5.5	38.0	1084.2	556.2	362.7	39.4	377.1	18.6	58.7	154.8
SD	2033.0	2458.8	49.0	7.4	15.8	1471.5	613.5	451.7	37.7	362.7	6.0	63.3	111.3
CV%	68.6	63.5	42.9	64.7	157.4	62.1	75.6	65.8	80.4	88.4	111.0	79.4	93.1
Summer													
Mean	1934.4	2091.5	41.4	7.4	8.9	1152.0	354.4	272.9	55.1	532.9	15.2	66.1	307.7
Median	1211.2	1446.4	8.1	4.2	4.6	698.3	188.0	190.2	27.6	324.6	10.5	49.1	180.0
SD	1875.8	1817.3	40.9	7.0	8.5	1017.7	340.5	243.0	50.7	446.6	11.2	55.4	271.7
CV%	62.6	69.2	19.5	56.5	52.0	60.6	53.1	69.7	50.1	60.9	69.1	74.2	58.5
Autumn													
Mean	2542.2	3830.1	86.6	15.3	107.0	2306.0	1491.5	394.5	131.8	810.7	69.5	126.7	365.2
Median	1787.6	2605.0	59.4	10.7	46.7	1962.2	832.2	276.0	102.7	587.7	47.3	95.9	310.9
SD	1962.3	3256.6	87.1	12.8	102.4	1717.4	1331.8	322.8	117.0	657.2	84.7	100.8	284.9
CV%	70.3	68.0	68.7	70.1	43.7	85.1	55.8	70.0	78.0	72.5	68.0	75.6	85.1
Winter													
Mean	3564.1	4300.4	98.5	50.1	17.7	2665.3	1362.6	1120.0	85.7	766.9	11.1	202.2	169.2
Median	2196.6	2349.5	87.3	20.6	10.4	1633.5	941.1	619.9	62.3	617.8	6.7	91.2	94.4
SD	3886.2	4896.2	51.6	123.9	31.4	2855.1	1372.4	1508.6	79.3	594.5	11.0	452.3	225.7
CV%	109.0	113.9	52.4	247.6	177.6	107.1	100.7	134.7	92.6	77.5	99.9	223.6	133.3
Annual													
Mean	2603.8	3362.7	69.0	20.5	39.9	1978.6	995.2	588.8	80.8	636.4	28.4	118.1	251.8
SD	2437.3	3146.2	47.7	64.8	52.2	1935.6	972.3	859.0	76.7	511.3	35.9	240.9	241.5

Abbreviations: SD, Standard deviation, CV, coefficient of variation.

Pingyao may be closely related to vehicle emissions and coal combustion (Wang et al., 2013).

3.3. Source distribution of heavy metals in $PM_{2.5}$

PCA was used to analyze the source distribution of the 13 heavy metals in this study. KMO and Bartlett's sphericity tests were performed to verify feasibility before PCA. The test results for spring (KMO = 0.697, $P < 0.001$), summer (KMO = 0.722, $P < 0.001$), autumn (KMO = 0.794, $P < 0.001$), and winter (KMO = 0.798, $P < 0.001$) showed that they were suitable for source identification analysis.

Spring: The four principal components explained 85.69 % of the total variables (Table S3). The Al, Ca, Fe, K, Mg, and Na loads in PC1 were very high. Al and Fe are crustal elements that originate mainly from nature (Zhao et al., 2019; Kong et al., 2010). According to the EF analysis results, the values of K, Mg, Na, and Ca were all less than five and mainly originated from nature, and PC1 might be interpreted as natural sources. PC2, with a contribution rate of 25.31 %, was mainly characterized by Zn, Pb, Cr, Mn, and Cu. The EF results showed that Cr and Mn were less affected by human activity. Banerjee et al. (2015) found that Pb, Cu, and Zn are mainly related to vehicle exhaust emissions, brake wear, and the use of leaded gasoline. In 2020, the number of civilian vehicles has reached 81,000 in Pingyao (PCBS, 2021). The sampling site was located in the center of the county with high motor traffic; therefore, PC2 was assigned as vehicle emissions. Only the Ni load of PC3 was >0.6; the moderate enrichment of Ni was related to the industrial sources of coal and oil combustion (Vallius et al., 2005), and PC3 might be related to industrial sources. PC4, with a contribution rate of 12.18 %, was mainly characterized by Co. The EF of Co has reached the level of severe enrichment, which is mainly produced by human activities, Liu et al. (2019) showed that Co was released during the combustion of fossil fuels such as coal and oil. In 2020, the output of coal-fired power generation has reached 2.12 billion KWH in Pingyao (PCBS, 2021). Therefore, PC4 could be allocated to coal combustion. **Summer:** PC1, with a contribution rate of 53.37 %, was mainly characterized by Al, Ca, Fe, K, and Mg. PC1 was considered natural source. In PC2, the highest loads were observed for Zn, Mn, and Pb. The release of Zn and Pb was closely related to vehicle emissions. PC2 was assigned to vehicle emissions. The loads of Co and Ni in PC3 are >0.6. When Co and Ni are distributed in the same component, it is generally considered to be related to the industrial production activities consuming fossil energy (Liu et al., 2018), PC3 might be allocated to industry sources. **Autumn:** PC1, with a contribution rate of 55.84 %, was mainly characterized by Al, Ca, Co, Cr, Fe, Mg, Mn, and Zn. The EF results showed that Co mainly originated from human production activities, while other elements were greatly affected by natural sources. Thus, PC1 may be interpreted as a natural and coal-burning source. In PC2, the highest loads were observed for K, Ni, and Na. Na and K are the identification elements of biomass combustion (Simoneit et al., 1999; Begum et al., 2004). Some autumn samples were collected during the harvest period. Agricultural waste burning still exists despite measures introduced by the local government to target crop burning. Therefore, PC2 was assigned to biomass burning. PC3 may be allocated to vehicle emissions. **Winter:** PC1, with a contribution rate of 48.58 %, was mainly characterized by Al, Ca, Fe, K, Mg, and Mn. Thus, PC1 may be interpreted as a natural source. PC2 may be related to vehicle emissions. PC3 was determined to correspond to coal combustion.

The analytical results in autumn were significantly different from those in other seasons, which can be attributed to two reasons. First, there might be a mixed discharge of multiple pollution sources in Pingyao in autumn, which leads to the accumulation of pollutants under adverse meteorological conditions and brings more uncertainty to source identification. Second, autumn agricultural production activities in Pingyao were mainly concentrated one week before the sampling period, but crop burning still existed during the monitoring period, which may be the main reason why biomass burning became a major source of pollution. In contrast, biomass burning cannot be identified as the dominant source in other seasons due to the relative scarcity of biomass fuels and government monitoring. County towns try on arable land rather than urban centers. Since China has cleaned up straw burning in county-level units in recent years, a problem with agricultural waste incineration remains that we do not pay much more attention to county-level units than to cities.

3.4. Share of pollution sources

Based on PCA determination of the pollutant composition of heavy metals in $PM_{2.5}$ in four seasons, the APCS-MLR model was used to obtain the source distribution of each heavy metal, and further calculate the share of each potential pollutant source (Thurston and Spengler, 1985; Lv, 2019). The linear fitting of the predicted and measured concentrations

of heavy metals in $PM_{2.5}$ is shown in Fig. S1. Except for Na (0.678) and Pb (0.475), the R^2 values of most elements were between 0.773 and 0.962, indicating that the APCS-MLR model is reliable and the results are credible.

The source distribution of each heavy metal and the share of the pollution sources are shown in Fig. 3. Natural sources were the main sources of heavy metals in fine particulate matter during the spring and winter

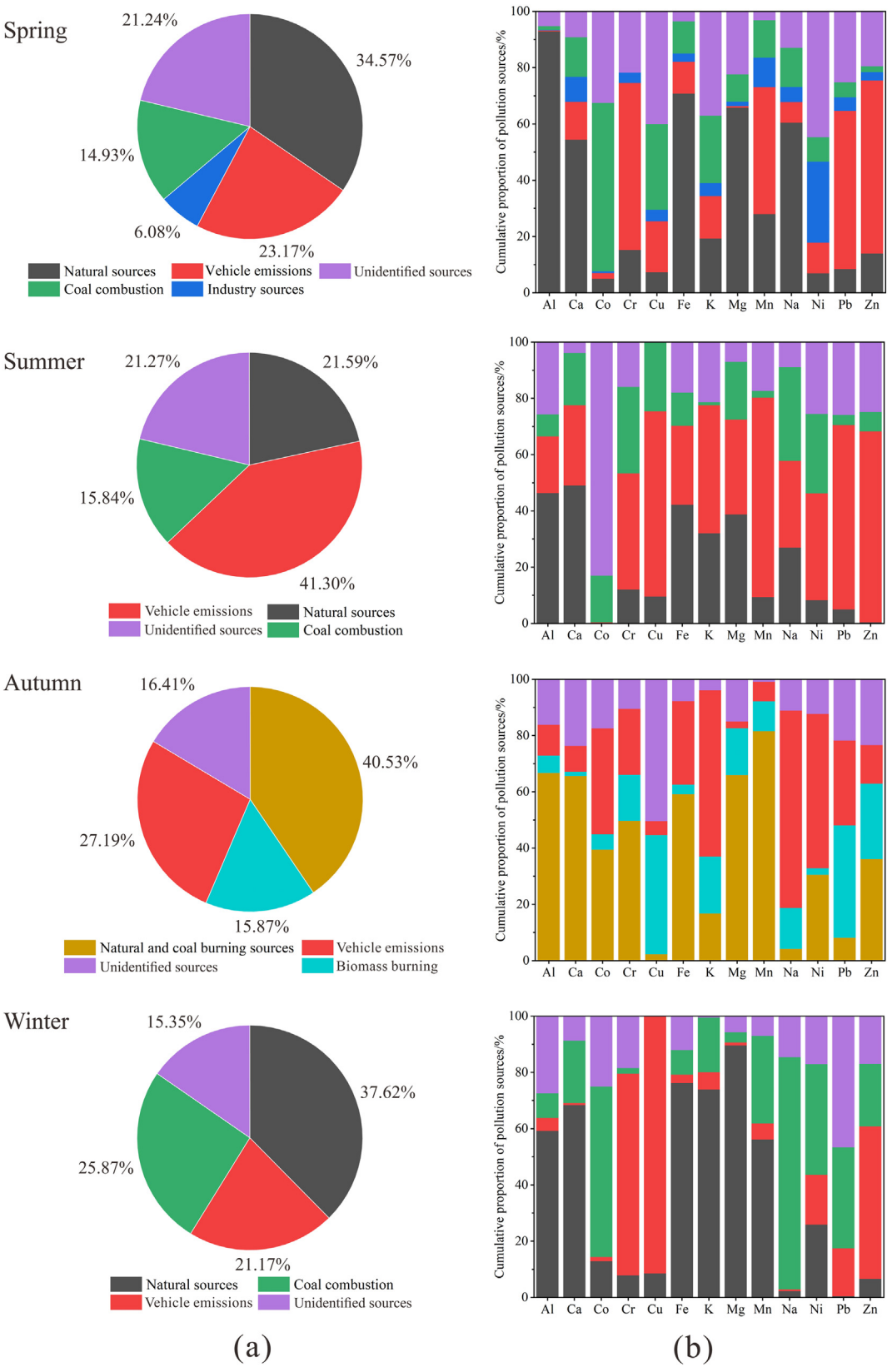

Fig. 3. Source distribution of heavy metals in $PM_{2.5}$ based on APCS-MLR model (a), and the distribution of pollution sources for each heavy metal (b).

monitoring periods, accounting for 34.57 % and 37.62 %, respectively, which was related to frequent sand-wind weather during this period. Strong winds might increase the burden of air pollution in Pingyao by carrying bare farmland soil and road dust around the sampling site (Peng et al., 2016; Yadav and Raman, 2021). Compared with other seasons, coal combustion pollution is higher in winter, and the heating activities of urban residents significantly increase the contribution rate of this source to air pollution (Ji et al., 2019). It is a remarkable fact that the contribution rate of vehicle emissions is higher in summer (41.30 %), which may be due to the fact that the summer monitoring period is in the peak tourism season, when the COVID-19 pandemic in China significantly improved. According to the Chinese Center for Disease Control and Prevention, there were no suspected or confirmed cases in Shanxi Province. Transportation had all returned to normal, with high human traffic leading to more vehicle emissions. The main source of pollution in autumn was a mixed source of natural and coal burning. Coal combustion is closely related to the coincidence of the atmospheric monitoring period and Pingyao heating time. However, biomass burning, a typical pollution source in autumn, contributed the least to heavy metals, accounting for only 15.87 %. According to the field survey, agricultural activities in autumn 2020 in Pingyao were mainly concentrated around October 9, while agricultural activities ended when atmospheric monitoring began, and the air pollutants produced by crop combustion were largely dispersed, which may be the main reason for the low contribution of biomass combustion.

3.5. Health risk assessment of heavy metals in $PM_{2.5}$

To verify that traditional health risk assessment models may underestimate or overestimate the health risks to all populations, traditional models and Monte Carlo simulation-based risk assessment models were used to calculate the non-carcinogenic risks of Pb to humans in autumn. The results of the traditional model showed that Pb might have a non-carcinogenic risk in children (HQ = 1.14) but has no effect on adults (HQ = 0.28). However, Pb only had potential risks for 37.69 % of children through the Monte Carlo simulation, and the vast majority of children were still not affected by the health effects off Pb. In addition, 1.03 % of adults exposed to outdoor environments still need to consider the health effects of Pb. The health risk assessment model using Monte Carlo simulation can avoid underestimation and overestimation of health risks and significantly improve the reliability of health risk assessment.

3.5.1. Health risk assessment based on probability distribution

A Monte Carlo simulation was used to evaluate the carcinogenic and non-carcinogenic risk probabilities of populations (including children and adults) exposed to heavy metals in fine particulate matter in Pingyao in three different ways, and the results are shown in Table S6-S9. The probability distributions of non-carcinogenic risks HQ and HI for all populations are shown in Figs. S2–5. The average annual HQ of heavy metals, from large to small, was Pb > Cr > Co > Mn > Ni > Zn > Cu. The non-carcinogenic risk of children was greater than that of adults, and the high HQ value of Pb was the main reason for the increase in the non-carcinogenic risk of children. Crystal Ball software v11.1.24 (Oracle, USA) was used to run 10,000 simulations of four seasons of heavy metal HQ (Karami et al., 2019). The results showed that the HQ values of Ni, Zn, and Cu in adults were <1, and there were very few simulation results for Ni, Zn, and Cu being >1 in children, indicating that Ni, Zn, and Cu hardly pose a non-carcinogenic risk to human health. The HQ values of Pb, Cr, and Co were the highest in winter, the non-carcinogenic risk of Cu, Mn, and Ni reached a peak in autumn, and the non-carcinogenic risk of Zn was significantly higher in summer than in other seasons. An analysis of the four-season hazard index (HI) found that children had HI values >1 in four seasons (mean 2.17), while adults were only affected by non-carcinogenic risk in winter (winter = 1.08, mean = 0.63). The HI of heavy metals was significantly higher than the winter 2014 values for the Xinxiang urban area (adults 0.21, children 0.38) (Feng et al., 2017), the mean 2014–2020 values for the Shenzhen residential area (adults 0.41, children 0.3) (Yan et al., 2022), and the 2013–2014 Kunming industrial area (adults 0.17, children 0.26) (Han et al., 2021b), which indicated that the non-carcinogenic risk of heavy metals in fine particulate matter in the county of China was significantly higher than that in some large cities. Children, as the group most vulnerable to the non-carcinogenic risk of heavy metals in $PM_{2.5}$, should take the initiative to strengthen outdoor protection, especially in winter when the average HI is the highest, and Pb, Cr, and Co control should be prioritized.

The carcinogenic risk probability distribution of the four toxic heavy metals is presented in Figs. S2–5. The average annual CR values of Ni, Pb, Co, and Cr were 8.39E−05, 3.26E−06, 1.50E−07, 9.51E−08 for children, 5.30E−05, 2.06E−6, 1.23E−06, 1.38E−07 for adults. The CR values of Ni and Pb both exceeded the acceptable threshold of 1E−06. The potential carcinogenic risk of coal and other fossil energy emissions to local residents should be consider, especially in autumn. The carcinogenic risks of Ni for children and adults were 1.74E−04 and 1.08E−04 respectively, exceeding the limit of 1E−04, indicating that there was a serious carcinogenic risk. According to the results of the Monte Carlo simulation, the CR (Ni) of children and adults in autumn was 61.82 % and 37.56 % higher than that of 1E−04, respectively, and more than half of the children exposed to the outdoor environment were exposed to serious cancer risk. The annual mean total carcinogenic risk (TCR) for children and adults was 8.72E−05 and 5.64E−05 respectively, and peaked in autumn at 1.76E−04 and 1.11E−04, respectively. The health risk in children was significantly higher than that in adults. Compared with other cities in China, the TCR values of Pingyao were larger than those of Nanjing's educational and residential areas in spring 2013 (adults 2.71E−05, children 6.77E−06; adults 2.69E−05, children 6.73E−06) (Li et al., 2015), Jinan's urban area throughout 2016 (5.00 E−05) (Sui et al., 2020), the urban center of Baoding in spring 2016 (adults 5.66E−05, children 1.33E−06) (Lei et al., 2021), and lower than the typical urban functional area in Beijing in winter 2018 (adults 1.41E−04, children 2.59 E−04) (Fan et al., 2021). County−level residents in China were already more susceptible to cancer from pollution exposure than a few urban residents, and the health risks were even an order of magnitude higher. The health burden on approximately half of China's population must be considered seriously. The high health risk caused by $PM_{2.5}$ in autumn in Pingyao was closely related to the toxicity and human enrichment of Ni. Therefore, risk assessment undertaken in the atmospheric environment should pay closer attention to heavy metal exposure in children, especially for Pb, Cr, Co, and Ni.

3.5.2. Health risk assessment associated with pollution sources

Based on the results of the Monte Carlo simulation, the health risks caused by each pollution source were calculated by coupling the APCS-MLR model with the HRA model. To quantify the health risks posed by pollution sources to children and adults, the average health risks of individual heavy metals derived from Monte Carlo simulations were multiplied by the contribution rate of each potential pollution source (Ma et al., 2018). Health risks (non-carcinogenic and carcinogenic, Fig. 4) from different sources showed similar results in children and adults, which is consistent with the study results of Huang et al., 2021. The contribution of vehicle emissions to the non-carcinogenic risk for children and adults was much higher than that of unidentified sources, showing the same trend in spring, summer and winter. The non-carcinogenic risk of biomass burning due to frequent agricultural activities and large amounts of crop stacking and burning in autumn is as high as 35.17 % for adults and 27.51 % for children, indicating that biomass burning poses a significant health threat to adults. Vehicle emissions were a major source of non-carcinogenic risk for adults in winter, while children were more likely to originate from unidentified sources and from coal combustion. Unidentified sources may be a combination of various pollution sources with complex sources. It is difficult to achieve emission reduction of pollution sources through targeted control measures, making it difficult for children to protect their health during winter. For coal combustion, the high loads of Co and Na should be identified as priority pollutants for non-carcinogenic risk control in children.

The proportion of sources of cancer risk differed significantly across the four seasons. The carcinogenic risk to children and adults mainly came

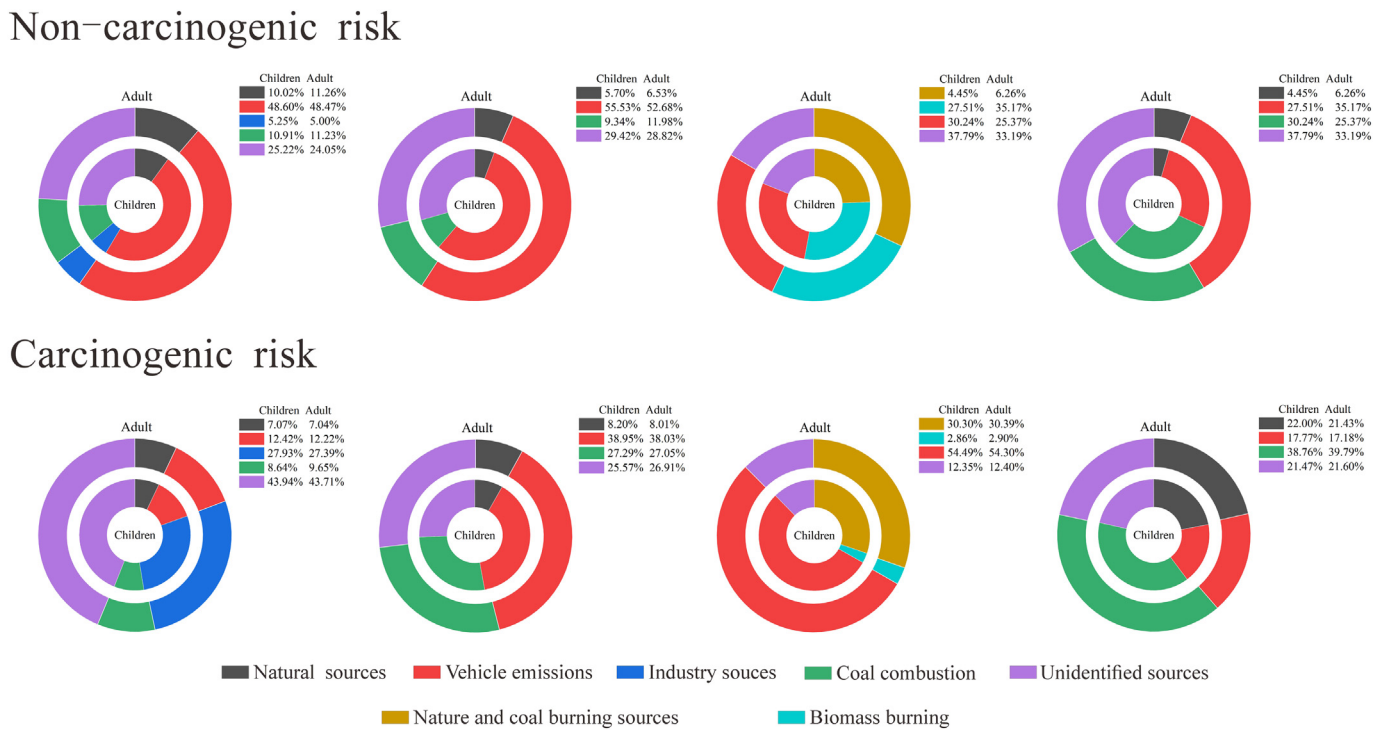

Fig. 4. Health risks to all groups from different sources of heavy metals.

from unidentified sources and industrial sources in spring, and the contribution rates of unidentified sources were 43.71 % and 43.94 %, respectively, which may be due to the mixed emissions of various potential pollution sources such as metal processing, coking, agricultural activities and biomass combustion (Fig. 3) (Ma et al., 2018). Therefore, joint management of multiple potential sources should be strengthened. In summer, vehicle emissions contribute the most to carcinogenic risk, followed by coal combustion, which is often overlooked. Summer is not the peak time for coal use, but the carcinogenic risk for children and adults from coal combustion was >27 %, which might be related to the increased use of coal during the peak power consumption in summer (Zhao et al., 2013; Tao et al., 2014; Gao et al., 2018). Urban power generation in Pingyao is mainly thermal power generation, and the raw materials used for thermal power generation are mainly coal and other fossil fuels. The source identification results show that the share of coal combustion was 15.84 % in summer, which is higher than 14.93 % in spring. In addition to the priority control of the indicative elements Zn, Mn, and Pb in vehicle emissions, the optimization of the regional energy utilization structure should also be promoted, strengthening power generation from clean energy sources such as solar and wind power, or improving the efficiency of coal combustion. The greatest contribution of vehicle emissions to human carcinogenic risk occurred in autumn, reaching 54.30 % for children and 54.49 % for adults. The high contribution from vehicle emissions was similar to that in summer. The proportion of biomass combustion in carcinogenic risk was much lower than that in non-carcinogenic risk; therefore, more attention should be paid to the impact of biomass combustion on the non-carcinogenic risk to humans. The carcinogenic risk of coal combustion caused by heating activities was the highest in winter. In general, $PM_{2.5}$-bound heavy metals from vehicle emissions and coal combustion were the primary causes of the increased health burden on the population in Pingyao. Prevention and treatment of health concerns in county-level units should proceed as planned.

The health problem of population exposure to $PM_{2.5}$ in Chinese county-level units is extremely severe. Counties are likely to suffer from higher air pollution than urban areas in the coming decades, and the focus of future research should gradually shift from cities to counties (Su, 2021; Li et al., 2019). Atmospheric heavy metal pollution prevention and control policies formulated by the government should be targeted, and the promotion of new energy vehicles and the gradual replacement of fossil energy sources, such as coal, by clean energy sources will remain the major control measures to reduce the health risks to the population in the future.

3.6. Strengths and limitations

Our survey sampling covered four seasons, which can comprehensively characterize the annual variation in population health risk in county-level units. Additionally, probabilistic simulation and source-based health risk assessment tools can accurately quantify the health burden of population exposure to heavy metals in $PM_{2.5}$. Nevertheless, our research in only one county cannot represent the overall situation of county-level units in China. Future studies at larger spatial scales are needed to verify our views.

4. Conclusions

A comprehensive investigation was conducted to analyze the pollution characteristics, sources, and health risks of heavy metals in $PM_{2.5}$ in county-level units. The concentration of $PM_{2.5}$ was the highest in autumn, reaching 93.13 ± 53.33 μg/m^3, which was closely related to frequent artificial production activities during the monitoring period. Ca, Al, Fe, K, Na, and Mg, mainly from nature, were the most abundant metals in $PM_{2.5}$, but these ubiquitous metals do not endanger human health. Pb, Co, and Zn were greatly affected by anthropogenic production activities and were closely related to artificial source emissions. Seasonal differences were observed in the sources of the heavy metals in Pingyao.

Concentration-based and source-based health risks of heavy metals in $PM_{2.5}$ were evaluated, the non-carcinogenic risk caused by heavy metals in county-level units was significantly higher than that in some large cities. Children were more susceptible to heavy metals than adults, with a mean HI of 2.17 over the four seasons, reaching a maximum value of 3.58 in winter. The high HQ of Pb (mean value of 1.40) was the main reason for the increase in non-carcinogenic risk in children. County-level residents in China were already more susceptible to cancer from pollution exposure than a few urban residents, and the health risks were even an order of magnitude higher. Notably, all groups were at serious carcinogenic risk in autumn,

1.76E-04 for children and 1.11E-04 for adults. Ni control schemes should be considered because of their high carcinogenic risk. The health burden on approximately one in ten people worldwide must be taken seriously. The health risks of different pollution sources were similar in children and adults. Vehicle emissions and coal combustion should be considered the main sources of control to reduce the health risks posed by heavy metals in $PM_{2.5}$. Air pollution treatment is difficult in county-level units with large populations and wide areas of land. Preventing and managing health threats to the population in China's county-level units should be a primary concern in the future.

CRediT authorship contribution statement

Wenju Wang, Chun Chen, Dan Liu: Investigation, Conceptualization, Writing, Formal analysis, Data Curation and Editing.

Mingshi Wang, Qiao Han, Xuechun Zhang: Conceptualization, Methodology, Supervision, Project administration and Review.

Xixi Feng, Ang Sun, Pan Mao: Investigation, Experimental analysis, Data Curation, Review.

Qinqing Xiong, Chunhui Zhang: Experimental analysis, Data Curation, Investigation and Experimental analysis.

Declaration of competing interest

The authors declare that they have no known competing financial interests or personal relationships that could have appeared to influence the work reported in this paper.

Acknowledgments

This work was supported by the National Natural Science Foundation of China (42177070): Migration processes of pathogenic bacteria at the subsurface media interface in livestock manure return areas and their driving mechanisms.

Appendix A. Supplementary data

Supplementary data to this article can be found online at https://doi.org/10.1016/j.scitotenv.2022.156777.

References

Abuduwailil, J., Zhaoyong, Z., Fengqing, J., 2015. Evaluation of the pollution and human health risks posed by heavy metals in the atmospheric dust in Ebinur Basin in Northwest China. Environ. Sci. Pollut. Res. 22, 14018–14031. https://doi.org/10.1007/s11356-015-4625-1.

Banerjee, T., Murari, V., Kumar, M., Raju, M.P., 2015. Source apportionment of airborne particulates through receptor modeling: Indian scenario. Atmos. Res. 164–165, 167–187. https://doi.org/10.1016/j.atmosres.2015.04.017.

Beelen, R., Hoek, G., Raaschou-Nielsen, O., Stafoggia, M., Andersen, Z.J., Weinmayr, G., et al., 2015. Natural-cause mortality and long-term exposure to particle components: an analysis of 19 european cohorts within the multi-center ESCAPE project. Environ. Health Perspect. 123, 525–533. https://doi.org/10.1289/ehp.1408095.

Begum, B.A., Kim, E., Biswas, S.K., Hopke, P.K., 2004. Investigation of sources of atmospheric aerosol at urban and semi-urban areas in Bangladesh. Atmos. Environ. 38, 3025–3038. https://doi.org/10.1016/j.atmosenv.2004.02.042.

Cao, J., Xu, H., Xu, Q., Chen, B., Kan, H., 2012. Fine particulate matter constituents and cardiopulmonary mortality in a heavily polluted Chinese City. Environ. Health Perspect. 120, 373–378. https://doi.org/10.1289/ehp.1103671.

Chen, R., Chen, H., Song, L., Yao, Z., Meng, F., Teng, Y., et al., 2019a. Characterization and source apportionment of heavy metals in the sediments of Lake Tai (China) and its surrounding soils. Sci. Total Environ. 694, 133819. https://doi.org/10.1016/j.scitotenv.2019.133819.

Chen, B., Wang, X.B., Li, Y.L., Yang, Q., Li, J.S., 2019b. Energy-induced mercury emissions in global supply chain networks: structural characteristics and policy implications. Sci. Total Environ. 670, 87–97. https://doi.org/10.1016/j.scitotenv.2019.03.215.

Chen, C., Zhu, P., Lan, L., Zhou, L., Liu, R., Sun, Q., et al., 2018. Short-term exposures to PM2.5 and cause-specific mortality of cardiovascular health in China. Environ. Int. 161, 188–194. https://doi.org/10.1016/j.envres.2017.10.046.

Cohen, A.J., Brauer, M., Burnett, R., Anderson, H.R., Frostad, J., Estep, K., et al., 2017. Estimates and 25-year trends of the global burden of disease attributable to ambient air pollution: an analysis of data from the global burden of diseases study 2015. Lancet 391, 1907–1918. https://doi.org/10.1016/S0140-6736(17)30505-6.

Copat, C., Cristaldi, A., Fiore, M., Grasso, A., Zuccarello, P., Signorelli, S.S., et al., 2020. The role of air pollution (PM and NO2) in COVID-19 spread and lethality: a systematic review. Environ. Res. 191, 110129. https://doi.org/10.1016/j.envres.2020.110129.

Cristaldi, A., Fiore, M., Conti, G.O., Pulvirenti, E., Favara, C., Grasso, A., et al., 2022. Possible association between PM2.5 and neurodegenerative diseases: a systematic review. Environ. Res. 208, 112581. https://doi.org/10.1016/j.envres.2021.112581.

Dastoorpoor, M., Sekhavatpour, Z., Masoumi, K., Mohammadi, M.J., Aghababaeian, H., Khanjani, N., et al., 2019. Air pollution and hospital admissions for cardiovascular diseases in Ahvaz, Iran. Sci. Total Environ. 652, 1318–1330. https://doi.org/10.1016/j.scitotenv.2018.10.285.

Dong, Y., Zhou, H., Fu, Y., Li, X., Geng, H., 2021. Wavelet periodic and compositional characteristics of atmospheric PM2.5 in a typical air pollution event at Jinzhong city, China. Atmos. Pollut. Res. 12, 245–254. https://doi.org/10.1016/j.apr.2020.09.013.

Fan, M.Y., Zhang, Y.L., Lin, Y.C., Cao, F., Sun, Y., Qiu, Y., 2021. Specific sources of health risks induced by metallic elements in PM2.5 during the wintertime in Beijing, China. Atmos. Environ. 246, 118112. https://doi.org/10.1016/j.atmosenv.2020.118112.

Feng, J., Yu, H., Liu, S., Su, X., Li, Y., Pan, Y., et al., 2017. PM2.5 levels, chemical composition and health risk assessment in Xinxiang, a seriously air-polluted city in North China. Environ. Geochem. Health 39, 1071–1083. https://doi.org/10.1007/s10653-016-9874-5.

Feng, J., Yu, H., Mi, K., Su, X., Li, Y., Li, Q., et al., 2018. One year study of PM2.5 in Xinxiang city, North China: seasonal characteristics, climate impact and source. Ecotoxicol. Environ. Saf. 154, 75–83. https://doi.org/10.1016/j.ecoenv.2018.01.048.

Fryer, M., Collins, C.D., Ferrier, H., Colvile, R.N., Nieuwenhuijsen, M.J., 2006. Human exposure modelling for chemical risk assessment: a review of current approaches and research and policy implications. Environ. Sci. Policy. 9, 261–274. https://doi.org/10.1016/j.envsci.2005.11.011.

Gao, J., Wang, K., Wang, Y., Liu, S., Zhu, C., Hao, J., et al., 2018. Temporal-spatial characteristics and source apportionment of PM2.5 as well as its associated chemical species in the Beijing-Tianjin-Hebei region of China. Environ. Pollut. 233, 714–724.

Ghasemi, F.F., Dobaradaran, S., Saeedi, R., Nabipour, I., Nazmara, S., Abadi, D.R.V., et al., 2020. Levels and ecological and health risk assessment of PM2.5-bound heavy metals in the northern part of the Persian Gulf. Environ. Sci. Pollut. Res. 27, 5305–5313. https://doi.org/10.1007/s11356-019-07272-7.

Gholizadeh, M.H., Melesse, A.M., Reddi, L., 2016. Water quality assessment and apportionment of contamination sources using APCS-MLR and PMF receptor modeling techniques in three major rivers of South Florida. Sci. Total Environ. 566–567, 1552–1567. https://doi.org/10.1016/j.scitotenv.2016.06.046.

Goudarzi, G., Alavi, N., Geravandi, S., Idani, E., Behrooz, H.R.A., Babaei, A.A., et al., 2018. Health risk assessment on human exposed to heavy metals in the ambient air PM10 in Ahvaz, Southwest Iran. Int. J. Biometeorol. 62, 1075–1083. https://doi.org/10.1007/s00484-018-1510-x.

Guo, D., Wang, R., Zhao, P., 2020a. Spatial distribution and source contributions of PM2.5 concentrations in Jincheng, China. Atmos. Pollut. Res. 11, 1281–1289. https://doi.org/10.1016/j.apr.2020.05.004.

Guo, Q., Li, L., Zhao, X., Yin, B., Liu, Y., Wang, X., et al., 2021. Source apportionment and health risk assessment of metal elements in PM2.5 in Central Liaoning's urban agglomeration. Atmosphere. 12, 667. https://doi.org/10.3390/atmos12060667.

Guo, W., Zhang, Z., Zheng, N., Luo, L., Xiao, H., Xiao, H., 2020b. Chemical characterization and source analysis of water-soluble inorganic ions in PM2.5 from a plateau city of Kunming at different seasons. Atmos. Res. 234, 104687. https://doi.org/10.1016/j.atmosres.2019.104687.

Hahad, O., Lelieveld, J., Birklein, F., Lieb, K., Daiber, A., Münzel, T., 2020. Ambient air pollution increases the risk of cerebrovascular and neuropsychiatric disorders through induction of inflammation and oxidative stress. Int. J. Mol. Sci. 21 (12), 4306. https://doi.org/10.3390/ijms21124306.

Han, X., Li, S., Li, Z., Pang, X., Bao, Y., Shi, J., et al., 2021b. Concentrations, source characteristics, and health risk assessment of toxic heavy metals in PM2.5 in a Plateau City (Kunming) in Southwest China. Int. J. Environ. Res. Public Health 18 (21), 11004. https://doi.org/10.3390/ijerph182111004.

Han, Q., Wang, M., Cao, J., Gui, C., Liu, Y., He, X., et al., 2020. Health risk assessment and bioaccessibilities of heavy metals for children in soil and dust from urban parks and schools of Jiaozuo, China. Ecotoxicol. Environ. Saf. 191, 110157. https://doi.org/10.1016/j.ecoenv.2019.110157.

Han, C., Xu, R., Gao, C., Yu, W., Zhang, Y., Han, K., et al., 2021a. Socioeconomic disparity in the association between long-term exposure to PM2.5 and mortality in 2640 Chinese counties. Environ. Int. 146, 106241. https://doi.org/10.1016/j.envint.2020.106241.

Hu, B., Jia, X., Hu, J., Xu, D., Xia, F., Li, Y., 2017. Assessment of heavy metal pollution and health risks in the soil-plant-human system in the Yangtze River Delta, China. Int. J. Environ. Res. Public Health 14, 1042. https://doi.org/10.3390/ijerph182111004.

Huang, J., Wu, Y., Sun, J., Li, X., Geng, X., Zhao, M., et al., 2021. Health risk assessment of heavy metal(loid)s in park soils of the largest megacity in China by using Monte Carlo simulation coupled with positive matrix factorization model. J. Hazard. Mater. 415, 125629. https://doi.org/10.1016/j.jhazmat.2021.125629.

IARC, 2016. Agents Classified by the IARC Monographs. International Agency for Research on Cancer, pp. 1–129.

Idani, E., Geravandi, S., Akhzari, M., Goudarzi, G., Alavi, N., Yari, A.R., et al., 2020. Characteristics, sources, and health risks of atmospheric PM10-bound heavy metals in a populated middle eastern city. Toxin Rev. 39 (3), 266–274. https://doi.org/10.1080/15569543.2018.1513034.

Jena, S., Perwez, A., Singh, G., 2019. Trace element characterization of fine particulate matter and assessment of associated health risk in mining area, transportation routes and institutional area of Dhanbad, India. Environ. Geochem. Hlth. 41, 2731–3747. https://doi.org/10.1007/s10653-019-00329-z.

Ji, W., Wang, Y., Zhuang, D., 2019. Spatial distribution differences in PM2.5 concentration between heating and non-heating seasons in Beijing, China. Environ. Pollut. 248, 574–583. https://doi.org/10.1016/j.envpol.2019.01.002.

Jin, G., Fang, W., Shafi, M., Wu, D., Li, Y., Zhong, B., et al., 2019. Source apportionment of heavy metals in farmland soil with application of APCS-MLR model: A pilot study for restoration of farmland in Shaoxing City Zhejiang, China. Ecotoxicol. Environ. Saf. 184, 109495. https://doi.org/10.1016/j.ecoenv.2019.109495.

Karami, M.A., Fakhri, Y., Rezania, S., Alinejad, A.A., Mohammadi, A.A., Yousefi, M., et al., 2019. Non-carcinogenic health risk assessment due to fluoride exposure from tea consumption in Iran using Monte Carlo simulation. Int. J. Environ. Res. Public Health 16, 4261. https://doi.org/10.3390/ijerph16214261.

Kong, S., Han, B., Bai, Z., Chen, L., Shi, J., Xu, Z., 2010. Receptor modeling of PM2.5, PM10, and TSP in different seasons and long-range transport analysis at a coastal site of Tianjin, China. Sci. Total Environ. 408, 4681–4694. https://doi.org/10.1016/j.scitotenv.2010.06.005.

Kong, L., Tan, Q., Feng, M., Qu, Y., An, J., Liu, X., et al., 2020. Investigating the characteristics and source analyses of PM2.5 seasonal variations in Chengdu, Southwest China. Chemosphere 243, 125267. https://doi.org/10.1016/j.chemosphere.2019.125267.

Lai, S., Xie, Z., Song, T., Tang, J., Zhang, Y., Mi, W., et al., 2015. Occurrence and dry deposition of organophosphate esters in atmospheric particles over the northern South China Sea. Chemosphere 127, 195–200. https://doi.org/10.1016/j.chemosphere.2015.02.015.

Lei, W., Li, X., Zhang, L., Xu, J., Zhao, W., Liu, Z., 2021. Pollution characteristics and health risk assessment of heavy metals in PM2.5 collected in Baoding. Environ. Sci. 42, 38–44 (In Chinese).

Li, H., Wang, J., Wang, Q., Qian, X., Qian, Y., Yang, M., 2015. Chemical fractionation of arsenic and heavy metals in fine particle matter and its implications for risk assessment: a case study in Nanjing, China. Atmos. Environ. 103, 339–346. https://doi.org/10.1016/j.atmosenv.2014.12.065.

Li, X., Li, S., Xiong, Q., Yang, X., Qi, M., Zhao, W., et al., 2018. Characteristics of PM2.5 chemical compositions and their effect on atmospheric visibility in urban Beijing, China during the heating season. Int. J. Environ. Res. Public Health 15, 1924. https://doi.org/10.3390/ijerph15091924.

Li, T., Guo, Y., Liu, Y., Wang, J., Wang, Q., Sun, Z., et al., 2019. Estimating mortality burden attributable to short-term PM2.5 exposure: a national observational study in China. Environ. Int. 125, 245–251. https://doi.org/10.1016/j.envint.2019.01.073.

Li, F., Yan, J., Wei, Y., Zeng, J., Wang, X., Chen, X., et al., 2021. PM2.5-bound heavy metals from the major cities in China: spatiotemporal distribution, fuzzy exposure assessment and health risk management. J. Clean. Prod. 286, 124967. https://doi.org/10.1016/j.jclepro.2020.124967.

Liu, X.G., Li, J., Qu, Y., Han, T., Hou, L., Gu, J., et al., 2013. Formation and evolution mechanism of regional haze: a case study in the megacity Beijing, China. Atmos. Chem. Phys. 13, 4501–4514. https://doi.org/10.5194/acpd-12-16259-2012.

Liu, J., Chen, Y., Chao, S., Cao, H., Zhang, A., Yang, Y., 2018. Emission control priority of PM2.5-bound heavy metals in different seasons: a comprehensive analysis from health risk perspective. Sci. Total Environ. 644, 20–30. https://doi.org/10.1016/j.scitotenv.2018.06.226.

Liu, P., Zhang, Y., Wu, T., Shen, Z., Xu, H., 2019. Acid-extractable heavy metals in PM2.5 over Xi'an, China: seasonal distribution and meteorological influence. Environ. Sci. Pollut. Res. 26, 34357–34367. https://doi.org/10.1007/s11356-019-06366-6.

Lv, J., 2019. Multivariate receptor models and robust geostatistics to estimate source apportionment of heavy metals in soils. Environ. Pollut. 244, 72–83. https://doi.org/10.1016/j.envpol.2018.09.147.

Ma, W., Tai, L., Qiao, Z., Zhong, L., Wang, Z., Fu, K., et al., 2018. Contamination source apportionment and health risk assessment of heavy metals in soil around municipal solid waste incinerator: a case study in North China. Sci. Total Environ. 631–632, 348–357. https://doi.org/10.1016/j.scitotenv.2018.03.011.

Massey, D.D., Kulshrestha, A., Taneja, A., 2013. Particulate matter concentrations and their related metal toxicity in rural residential environment of semi-arid region of India. Atmos. Environ. 67, 278–286. https://doi.org/10.1016/j.atmosenv.2012.11.002.

Mohammadi, M.J., Yari, A.R., Saghazadeh, M., Sobhanardakani, S., Geravandi, S., Afkar, A., et al., 2018. A health risk assessment of heavy metals in people consuming Sohan in Qom, Iran. Toxin Rev. 37 (4), 278–286. https://doi.org/10.1080/15569543.2017.1362655.

Ogundele, L.T., Owoade, O.K., Hopke, P.K., Olise, F.S., 2017. Heavy metals in industrially emitted particulate matter in Ile-Ife, Nigeria. Environ. Res. 156, 320–325. https://doi.org/10.1016/j.envres.2017.03.051.

PCBS, 2021. Pingyao County 2020 National Economic and Social Development Statistical Bulletin. Pingyao County Bureau of Statistics.

Peng, X., Shi, G., Zheng, J., Liu, J., Shi, X., Jiao, X., et al., 2016. Influence of quarry mining dust on PM2.5 in a city adjacent to a limestone quarry: seasonal characteristics and source contributions. Sci. Total Environ. 550, 940–949. https://doi.org/10.1016/j.scitotenv.2016.01.195.

Qiao, T., Zhao, M., Xiu, G., Yu, J., 2016. Simultaneous monitoring and compositions analysis of PM1 and PM2.5 in Shanghai: implications for characterization of haze pollution and source apportionment. Sci. Total Environ. 557–558, 386–394. https://doi.org/10.1016/j.scitotenv.2016.03.095.

Ran, J., Yang, A., Sun, S., Han, L., Li, J., Guo, F., et al., 2020. Long-term exposure to ambient fine particulate matter and mortality from renal failure: a retrospective cohort study in Hong Kong, China. Am. J. Epidemiol. 189, 602–612. https://doi.org/10.1093/aje/kwz282.

SEPA, 1990. Background Contents on Elements of Soils in China. China Environmental Science Press, Beijing (In Chinese).

Simoneit, B.R.T., Schauer, J.J., Nolte, C.G., Oros, D.R., Elias, V.O., Fraser, M.P., et al., 1999. Levoglucosan, a tracer for cellulose in biomass burning and atmospheric particles. Atmos. Environ. 33, 173–182. https://doi.org/10.1016/S1352-2310(98)00145-9.

Su, H., 2021. Foundation, trend and promotion of county"s urbanization in China. Economist 5, 110–119 (In Chinese).

Sui, S., Ng, J., Gao, Y., Peng, C., He, C., Wang, G., 2020. Pollution characteristics and chronic health risk assessment of metals and metalloids in ambient PM2.5 in Licheng District, Jinan, China. Environ. Geochem. Health 42, 1803–1815. https://doi.org/10.1080/10807039.2019.1684184.

Tao, J., Gao, J., Zhang, L., Zhang, R., Che, H., Zhang, Z., et al., 2014. PM2.5 pollution in a megacity of southwest China: source apportionment and implication. Atmos. Chem. Phys. 14, 8679–8699. https://doi.org/10.5194/acp-14-8679-2014.

Thurston, G.D., Spengler, J.D., 1985. A quantitative assessment of source contributions to inhalable particulate matter pollution in metropolitan Boston. Atmos. Environ. 19, 9–25. https://doi.org/10.1016/0004-6981(85)90132-5.

USEPA, 2011. Exposure Factors Handbook 2011 Edition (Final). U.S. Environmental Protection Agency, Washington, D.C.

Vallius, M., Janssen, N.A.H., Heinrich, J., Hoek, G., Ruuskanen, J., Cyrys, J., et al., 2005. Sources and elemental composition of ambient PM2.5 in three european cities. Sci. Total Environ. 337, 147–162. https://doi.org/10.1016/j.scitotenv.2004.06.018.

Wang, J., Hu, Z., Chen, Y., Chen, Z., Xu, S., 2013. Contamination characteristics and possible sources of PM10 and PM2.5 in different functional areas of Shanghai, China. Atmos. Environ. 68, 221–229. https://doi.org/10.1016/j.atmosenv.2012.10.070.

Wang, N., Zhao, X., Wang, J., Yin, B., Geng, C., Niu, D., et al., 2020. Chemical composition of PM2.5 and its impact on inhalation health risk evaluation in a City with light industry in Central China. Atmosphere. 11, 340. https://doi.org/10.3390/atmos11040340.

Xie, Y., Liu, Z., Wen, T., Huang, X., Liu, J., Tang, G., et al., 2019. Characteristics of chemical composition and seasonal variations of PM2.5 in Shijiazhuang, China: impact of primary emissions and secondary formation. Sci. Total Environ. 677, 215–229. https://doi.org/10.1016/j.scitotenv.2019.04.300.

Xie, Y., Lu, H., Yi, A., Zhang, Z., Zheng, N., Fang, X., et al., 2020. Characterization and source analysis of water–soluble ions in PM2.5 at a background site in Central China. Atmos. Res. 239, 104881. https://doi.org/10.1016/j.atmosres.2020.104881.

Yadav, K., Raman, R.S., 2021. Size-segregated chemical source profiles and potential health impacts of multiple sources of fugitive dust in and around Bhopal, Central India. Environ. Pollut. 284, 117385. https://doi.org/10.1016/j.envpol.2021.117385.

Yan, D., Lei, Y., Shi, Y., Zhu, Q., Li, L., Zhang, Z., 2018. Evolution of the spatiotemporal pattern of PM2.5 concentrations in China – a case study from the Beijing-Tianjin-Hebei region. Atmos. Environ. 183, 225–233. https://doi.org/10.1016/j.atmosenv.2018.03.041.

Yan, R.H., Peng, X., Lin, W., He, L.Y., Wei, F.H., Tang, M.X., et al., 2022. Trends and challenges regarding the source-specific health risk of PM2.5-bound metals in a Chinese megacity from 2014 to 2020. Environ. Sci. Technol. https://doi.org/10.1021/acs.est.1c06948.

Yang, S., Zhao, J., Chang, X.S., Collins, C., Xu, J., Liu, X., et al., 2019. Status assessment and probabilistic health risk modeling of metals accumulation in agriculture soils across China: a synthesis. Environ. Int. 128, 165–174. https://doi.org/10.1016/j.envint.2019.04.044.

Ye, L., Huang, M., Zhong, B., Wang, X., Tu, Q., Sun, H., et al., 2018. Wet and dry deposition fluxes of heavy metals in Pearl River Delta region (China): characteristics, ecological risk assessment, and source apportionment. J. Environ. Sci. (China) 70, 106–123. https://doi.org/10.1016/j.jes.2017.11.019.

Zhang, Y., Ji, X., Ku, T., Li, G., Sang, N., 2016. Heavy metals bound to fine particulate matter from northern China induce season-dependent health risks: a study based on myocardial toxicity. Environ. Pollut. 216, 380–390. https://doi.org/10.1016/j.envpol.2016.05.072.

Zhang, J., Zhou, X., Wang, Z., Yang, L., Wang, J., Wang, W., 2018. Trace elements in PM2.5 in Shandong Province: source identification and health risk assessment. Sci. Total Environ. 621, 558–577. https://doi.org/10.1016/j.scitotenv.2017.11.292.

Zhang, M., Li, Z., Xu, M., Yue, J., Cai, Z., Yung, K.K.L., 2019. Pollution characteristics, source apportionment and health risks assessment of fine particulate matter during a typical winter and summer time period in urban Taiyuan China. Hum. Ecol. Risk. Assess. 26, 2737–2750. https://doi.org/10.1080/10807039.2019.1684184.

Zhang, H., Cheng, S., Li, H., Fu, K., Xu, Y., 2020. Groundwater pollution source identification and apportionment using PMF and PCA-APCA-MLR receptor models in a typical mixed land-use area in southwestern China. Sci. Total Environ. 741, 140383. https://doi.org/10.1016/j.scitotenv.2020.140383.

Zhao, P.S., Dong, F., He, D., Zhao, X.J., Zhang, X.L., Zhang, W.Z., et al., 2013. Characteristics of concentrations and chemical compositions for PM2.5 in the region of Beijing, Tianjin, and Hebei, China. Atmos. Chem. Phys. 13, 4631–4644. https://doi.org/10.5194/acp-13-4631-2013.

Zhao, Z., Lv, S., Zhang, Y., Zhao, Q., Shen, L., Xu, S., et al., 2019. Characteristics and source apportionment of PM2.5 in Jiaxing, China. Environ. Sci. Pollut. Res. 26, 7497–7511. https://doi.org/10.1016/j.scitotenv.2019.133819.

Zhi, G., Zhang, Y., Sun, J., Cheng, M., Dang, H., Liu, S., et al., 2017. Village energy survey reveals missing rural raw coal in northern China: significance in science and policy. Environ. Pollut. 223, 705–712. https://doi.org/10.1016/j.envpol.2017.02.009.